



A concise SAR-analysis of antimicrobial cationic amphipathic barbiturates for an improved activity-toxicity profile

Manuel K. Langer^{a,1}, Aatur Rahman^{b,1}, Hymonti Dey^b, Trude Anderssen^c, Francesco Zilioli^a, Tor Haug^b, Hans-Matti Blencke^b, Klara Stensvåg^b, Morten B. Strøm^{c,**}, Annette Bayer^{a,*}

^a Department of Chemistry, UiT The Arctic University of Norway, NO-9037, Tromsø, Norway

^b The Norwegian College of Fishery Science, Faculty of Biosciences, Fisheries and Economics, UiT The Arctic University of Norway, NO-9037, Tromsø, Norway

^c Department of Pharmacy, Faculty of Health Sciences, UiT The Arctic University of Norway, NO-9037, Tromsø, Norway

ARTICLE INFO

Keywords:

Antibacterial
Barbiturates
Peptidomimetics
SMAMPs
Synthetic mimics of antimicrobial peptides

ABSTRACT

An amphipathic barbiturate mimic of the marine eusynstyelamides is reported as a promising class of antimicrobial agents. We hereby report a detailed analysis of the structure-activity relationship for cationic amphipathic *N,N'*-dialkylated-5,5-disubstituted barbiturates. The influence of various cationic groups, hydrocarbon linkers and lipophilic side chains on the compounds' antimicrobial potency and haemolytic activity was studied. A comprehensive library of 58 compounds was prepared using a concise synthetic strategy. We found cationic amine and guanidyl groups to yield the highest broad-spectrum activity and cationic trimethylated quaternary amine groups to exert narrow-spectrum activity against Gram-positive bacteria. *n*-Propyl hydrocarbon linkers proved to be the best compromise between potency and haemolytic activity. The combination of two different lipophilic side chains allowed for further fine-tuning of the biological properties. Using these insights, we were able to prepare both, the potent narrow-spectrum barbiturate **8a** and the broad-spectrum barbiturates **111G**, **13jA** and **13jG**, all having low or no haemolytic activity. The guanidine derivative **111G** demonstrated a strong membrane disrupting effect in luciferase-based assays. We believe that these results may be valuable in further development of antimicrobial lead structures.

1. Introduction

Since the golden age of antibiotics, the developing rate of new agents has decreased notably, while antimicrobial resistance (AMR) has been rising to a global threat [1]. The prominence of this problem is well demonstrated by the World Health Organization (WHO) enacting a global action plan on fighting antimicrobial resistance [2]. While the action plan is focusing on a framework at many different levels, the need for potent antimicrobials stays. As the antibiotics employed for decades start to lose activity against resistant bacteria, several alternative approaches have been investigated. Among these are combination therapy [3,4], bacteriophage therapy [5], photodynamic therapy [6], antibacterial antibodies [7], phytochemicals [5], nanoparticles [8] and antimicrobial peptides [9,10].

From the above stated list, the short, cationic antimicrobial peptides (AMPs) are an intriguing class of compounds. They constitute the first

line of host defense in virtually all eukaryotic species including plants, mammals, insects, etc. [11] They generally feature between 20 and 50% hydrophobic residues and have an overall positive charge (+2 to +9) at neutral pH [12–14]. Their amphipathic nature is the basis of their most common mode of action, to permeabilize bacterial membranes. AMPs attach to the negatively charged cytoplasmic membrane by electrostatic interactions and subsequently disrupt the apolar bilayer with their hydrophobic part [15]. It is believed that due to these non-specific interactions, bacterial resistance is less likely to be induced [16]. This makes AMPs a promising group of compounds despite their generally lower activity compared to marketed antibiotics [17].

Despite these promising properties, the clinical application of peptide based drugs is often limited by their poor oral uptake and proteolytic instability [18]. Therefore, considerable efforts towards the development of synthetic AMP analogues have been made, cumulating in the development of a variety of different groups of analogues [19–27].

* Corresponding author.

** Corresponding author.

E-mail addresses: Morten.strom@uit.no (M.B. Strøm), Annette.bayer@uit.no (A. Bayer).

¹ Authors contributed equally to this work.

Focusing on small molecules, we have recently reported substituted barbituric acid derivatives [28], inspired by a family of marine natural products, the *eusynstyelamides*, [29,30] as peptidomimetics of AMPs. The lead structure **1aG** (Fig. 1) from our previous study [28] demonstrated good *in vitro* and *in vivo* activity as a proof of principle.

Encouraged by the *in vivo* activity of **1aG** we herein describe an in-depth SAR investigation to improve the potency and selectivity of these peptidomimetics. Several series of amphipathic barbiturates with systematically varying substituents were designed and synthesized. Our aim was to assess the qualitative influence of each structural component aside from the barbituric acid on the antimicrobial and haemolytic activity. Once the impact of each component is identified, improved narrow- and broad-spectrum compounds may be prepared. All new compounds were screened for activity against a panel of antibiotic susceptible strains to determine their minimal inhibitory concentration (MIC) values. Cytotoxicity was assessed by determining the EC₅₀ values for the lysis of human red blood cells (RBC). Promising candidates were investigated for their antibacterial mode of action (MoA), using three luciferase-based assays of the viability and integrity of the cytoplasmic inner and outer membrane of bacterial cells.

2. Results and discussion

2.1. Design of the study

To systematically study the influence of structural components of **1aG** [28] (Fig. 1) on the antibacterial and haemolytic activity, we devised several series of compounds based on the general structure shown in Fig. 2. All structures consisted of a central barbituric acid core, which was kept constant. Three structural parts were varied in the design of the compound library: (i) the cationic head groups (blue placeholder in Fig. 2) attached to the nitrogen atoms of the barbiturate core by (ii) a hydrocarbon linker chain (green placeholder) and (iii) the two lipophilic side chains (red placeholders) connected to the barbiturate C-5 carbon.

The influence of the cationic head groups (R; Fig. 2) was investigated by including 1° amines, methylated 2°, 3° and 4° amines and imine derivatives containing guanidino or pyridinium groups in the library design. The cationic groups were chosen based on the prospect of varying the interactions with bacterial membranes and their ability to cross the latter and accumulate in Gram-negative *Escherichia coli* (*E. coli*) [31,32]. Compounds with varying cationic groups are found in compound series 1.

The lipophilic side chains (Fig. 2) were hypothesized to influence the compounds' ability to insert into the hydrophobic lipid bilayer of the bacteria. In our library design haloaryls, hetero-aryls, and linear and cyclic hydrocarbons were chosen as lipophilic side chains. The selection was based on results from our previous study [28] and commercial availability. Two different compound series were included in the study; in series 2 the two lipophilic side chains were identical, while in series 3 two different lipophilic side chains were combined resulting in

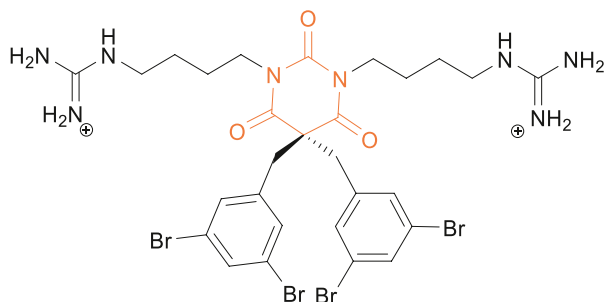


Fig. 1. Lead structure **1aG** from our previous study [28] with the barbituric acid core highlighted in orange.

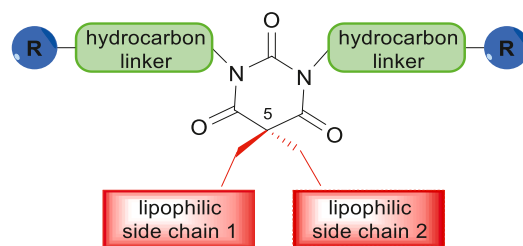


Fig. 2. General structure of the tetrasubstituted barbituric acids used in this study. R = cationic group. The individual parts were evaluated in five series, namely screening of the cationic moieties (series 1), lipophilic side chains (series 2 side chain 1 = side chain 2 and series 3 side chain 1 ≠ side chain 2), hydrocarbon linker chains (series 4) and optimized structures (series 5).

derivatives with mixed side chains.

The hydrocarbon linkers (Fig. 2) were chosen on the premises of investigating the influence of the flexibility and distance of the cationic groups relative to the barbiturate core. Linear hydrocarbon chains of 2–6 carbons length gave flexible linkers, while cyclic hydrocarbon linkers (cyclobutyl and cyclohexyl) gave more restricted analogues. Compounds with varying linkers are included in series 4.

Based on the results from series 4 we prepared a range of compounds included in series 5, having *n*-propyl linkers.

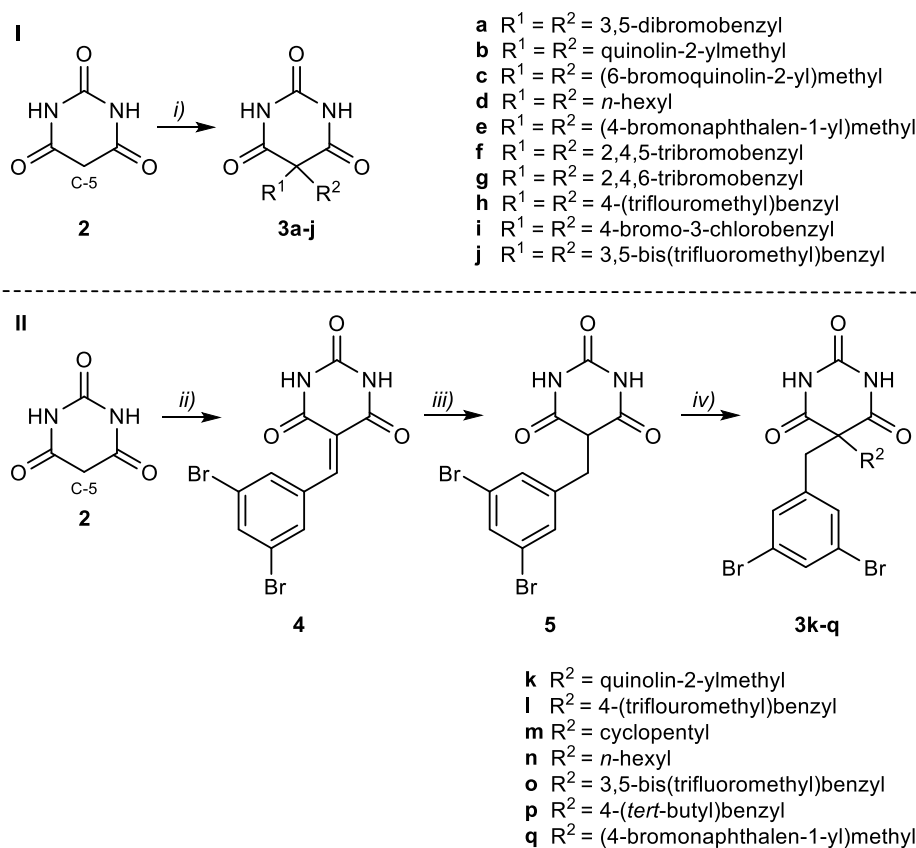
2.2. Synthesis

Our previously reported synthesis of 5,5-dialkylated barbiturates provided amine and guanidine analogues in six or eight synthetic steps, respectively [28]. In the present study, the demand for a large library of compounds prompted us to develop a shorter synthetic approach. Both amines and guanidines were successfully obtained in three steps from barbituric acid.

The synthetic strategy started with the preparation of symmetrical (**3a-j**) or unsymmetrical (**3k-q**) 5,5-dialkylated barbituric acid (Scheme 1). For the preparation of identically dialkylated compounds, barbituric acid **2** could be di-substituted at the C-5 carbon using organohalides to give **3a-j** in 5–92% yield in the presence of NaHCO₃ in PEG-400 (Scheme 1-I). Low yields (5–35%) were obtained for primary alkyl halides and heteroaryls, whereas haloaryls delivered good to excellent yields (70–92%). PEG-400 served as a green solvent alternative and phase transfer catalyst [33]. Commonly applied conditions [34] employing an inorganic base such as K₂CO₃ and benzyltriethylammonium chloride (BTEAC) in CHCl₃ performed worse. Weak electrophiles, such as alkyl halides posed an inherent problem. Harsher conditions were needed, which inevitably led to additional *N*-alkylation due to the acidity of the *N*-H protons (pK_a = 7–9 [35,36] compared to the pK_a (H-C5) = 3–4 [36, 37]).

To obtain unsymmetrically 5,5-dialkylated barbituric acids **3k-q** a different approach was needed, since mono-alkylation enhances the nucleophilicity of the barbiturate C-5 carbon leading to inevitable dialkylation [37]. We investigated several reported methods for selective monoalkylation and *in situ* reductions [37–39], which did not work well in our hands. We therefore decided to use a stepwise approach as shown in Scheme 1-II. Barbituric acid **2** and 3,5-dibromobenzaldehyde were condensed [40] to give compound **4** and subsequent reduction with NaBH₄ in EtOH [41] gave the C-5 mono-substituted derivative **5** in 80% yield. We found **5** being an approximate 2:1 mixture of the keto and enol form. This mixture was alkylated a second time using the conditions employed for 5,5-dialkylation of barbituric acid to deliver intermediates **3k-q**. Yields ranged from 5 to 61%, depending on the reactivity of the employed electrophiles.

Starting from intermediates **3**, a wide range of *N,N'*-dialkylated barbituric acid derivatives were prepared, employing a range of methods for *N*-alkylation depending on the availability of reactants



Scheme 1. Synthesis of core structures **3a–q**. **I**: Reaction conditions: i) Alkylating agent, NaHCO_3 , PEG-400, 45–100 °C, 5–92%. **II**: Reaction conditions: ii) 3,5-dibromobenzaldehyde, $\text{H}_2\text{O}/\text{EtOH}$ (3:1), 105 °C, 58%; iii) NaBH_4 , EtOH, 70 °C, 80%; iv) Alkyl bromide, NaHCO_3 , PEG-400, 50–100 °C, 5–61%.

(Scheme 2).

All compounds synthesized are summarized in Tables 1–5. Compounds denoted with capital **A** have an amine as a cationic group and those denoted with capital **G** have cationic guanidino groups, correspondingly. The compounds are grouped into five series (*series 1–5*) based on their structural variations.

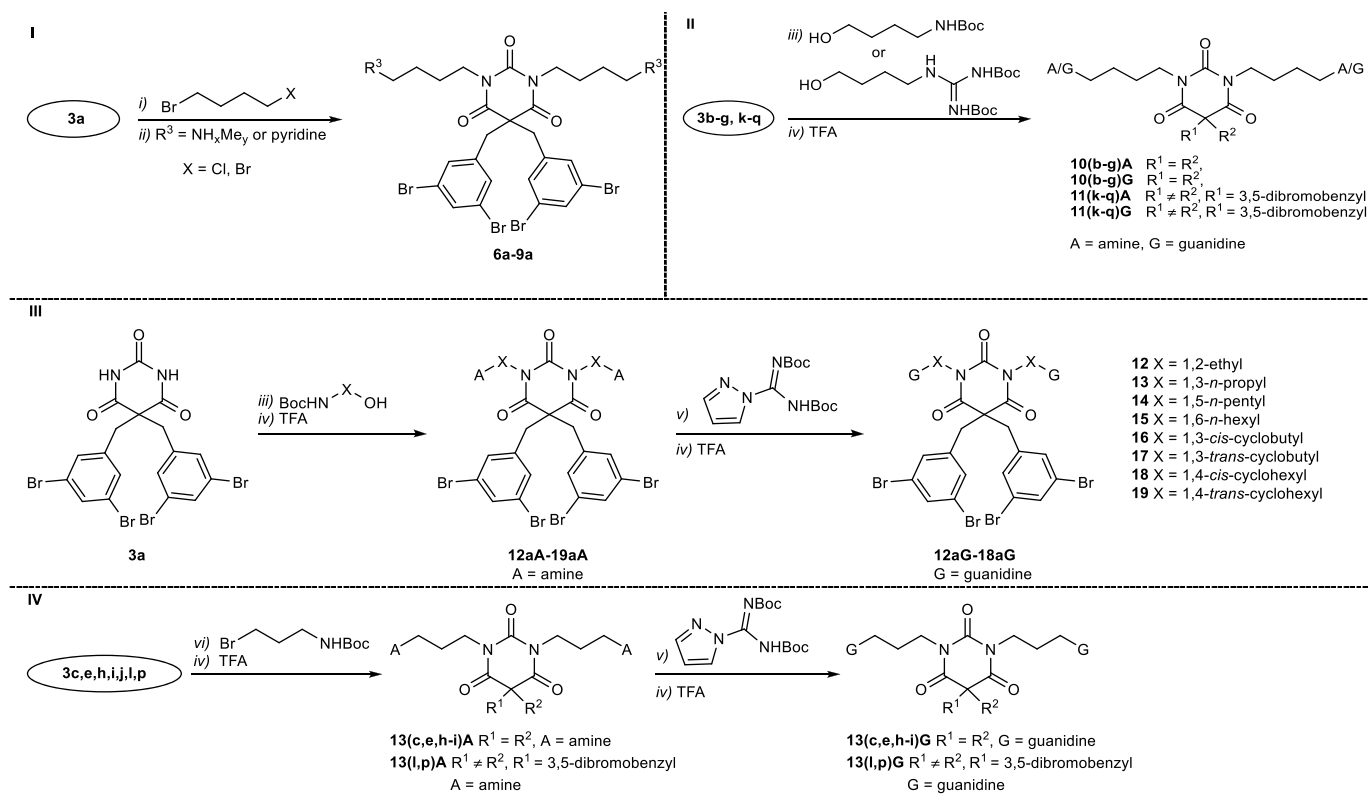
Series 1 (Table 1) encompasses compounds with varying cationic groups, while the C-5 substituents (3,5-dibromobenzyl) and hydrocarbon linker (*n*-butyl) were kept unchanged. To obtain the methylated amines and pyridinium containing compounds **6a–9a**, 5,5-bis(3,5-dibromobenzyl)barbituric acid **3a** was *N,N'*-dialkylated with either 1-bromo-4-chlorobutane or 1,4-dibromobutane and Cs_2CO_3 in acetone (Scheme 2-I). Subsequent $\text{S}_{\text{N}}2$ substitution of the terminal halo substituent with methylated ammonia or pyridine in acetonitrile at elevated temperature led to compounds **6a–9a** in 33–88% yield. Having a bromide as leaving group proved to be necessary for substitution with methylamine and dimethylamine. Substitutions were only successful with organic solutions of the amines, while hydrohalo salts of the amines could not be used. An optimized method for preparation of the previously reported 1° amine **1aA** and guanidine **1aG** [28] is described in the next paragraph.

Compound *series 2* (Scheme 2-II) contained identically 5,5-disubstituted barbiturates and *series 3* (Scheme 2-II) contained unsymmetrically 5,5-disubstituted barbiturates, while the hydrocarbon linker for both series was a *n*-butyl chain. As cationic groups, both amino (**A**) or guanidino (**G**) groups were explored. Compounds were synthesized from the barbituric acid derivatives **3b–g** or **3k–q** by *N,N'*-dialkylation with *N*-Boc protected 4-aminobutanol or *N,N'*-di-Boc protected 1-(4-hydroxybutyl)guanidine (Scheme 2-II). Due to the low pK_a value of the imidic hydrogens [42] a Mitsunobu protocol using diisopropylazodicarboxylate (DIAD) and PPh_3 could be employed. Removal of the Boc protection mediated by TFA:DCM and subsequent reversed phase (RP)

chromatography gave target *series 2* ($R^1 = R^2$) and *series 3* ($R^1 \neq R^2$) as di-TFA salts in 20–89% yield. In some cases the TFA salts were contaminated with reduced DIAD, which could largely be removed by trituration with Et_2O . Interestingly, employment of the more reactive coupling system 1,1'-(azodicarbonyl)dipiperidine ADDP/ $\text{P}(n\text{-Bu})_3$ and *N,N,N',N'*-tetramethyldicarboxamide TMAD/ $\text{P}(n\text{-Bu})_3$ [42] led to lower yields and mono-alkylation.

Series 4 (Table 4) contained compounds with varying linkers, such as aliphatic chains with 2–6 carbons length as well as cyclic hydrocarbons. The C-5 substituents were set to 3,5-dibromobenzyl and the cationic groups were either amino (**A**) or guanidino (**G**) groups. As the relevant linkers were commercially available as *N*-Boc-amino alcohols, we decided to explore the above Mitsunobu protocol in a stepwise synthetic approach (Scheme 2-III). The 5,5-bis(3,5-dibromobenzyl)barbituric acid **3a** was *N,N'*-dialkylated with the appropriate Boc-protected amino alcohol using the Mitsunobu conditions followed by TFA:DCM treatment to obtain compounds **12aA–19aA** in 23–73% over 2 steps. Treatment of the amines **12aA–19aA** with *N,N'*-Di-Boc-1*H*-pyrazole-1-carboxamide and DIPEA or DBU, followed by Boc removal with TFA in DCM delivered the guanidines **12aG–18aG** in 14–92% yield. Employing the well-known and cheaper alternative *N,N'*-bis(*tert*-butoxycarbonyl)-*S*-methylisothiourea [43,44] led to an inseparable mixture of Boc protected amine and Boc protected guanyl compounds.

Based on the bioactivities observed for *series 1–4*, a fifth collection of compounds (*series 5*, Table 5), exploring the effect of an *n*-propyl linker more broadly, was prepared. *Series 5* contained selected identically (*series 2*) or unsymmetrically (*series 3*) 5-substituted barbiturates with both 1-propyl-3-amino (**A**) or 1-propyl-3-guanidino groups (**G**) as *N,N'*-substituents. Starting from compounds **3c**, **e**, **h**, **i**, **j**, **l**, **p**, *N,N'*-alkylation with *N*-Boc *n*-propylbromide, followed by TFA mediated Boc removal and purification by RP chromatography gave identically **13(c,e,h,i,j)A**



Scheme 2. Synthetic approach to target series 1–5, where **A** denotes amine head groups and **G** the guanidine derivatives. All final compounds were obtained as di-TFA salts. I $R^3 = NH_2Me, NHMe_2, NMe_3, \text{pyridinyl}$; Reaction conditions: i) CS_2CO_3 , acetone, $55^\circ C$, 57–85%; ii) MeCN, $70\text{--}90^\circ C$, 33–88%. II Reaction conditions: iii) DIAD, PPh_3 , anhydrous DCM or THF, $0^\circ C$ to r.t., iv) TFA, DCM, r.t., 20–89% o2s. III Reaction conditions: iii) DIAD, PPh_3 , anhydrous DCM or THF, $0^\circ C$ to r.t., iv) TFA, DCM, r.t., 23–73% o2s, v) DIPEA or DBU, THF, $45^\circ C$, 14–92% o2s (after TFA deprotection). IV Reaction conditions: vi) base, TBAI, acetone, $50\text{--}70^\circ C$, then iv) TFA, DCM, r.t., 34–76% o2s (after TFA deprotection); v) DIPEA or DBU, THF, $45^\circ C$, then iv) TFA, DCM, r.t., 20–91% o2s (after TFA deprotection).

Table 1

Antimicrobial activity (MIC in $\mu g/mL$) against bacterial reference strains and haemolytic activity against human RBC (EC_{50} in $\mu g/mL$) for compounds in series 1.

Core structure	Comp. ID	R^3	CLogP ^a	Antimicrobial activity				EC_{50}^b
				S. a	B. s	E. c	P. a	
	1aG ^c		−2.39	2	2	2	8	62
	1aA ^d		−1.20	4	2	4	8	79
	6a		−0.66	8	4	8	16	73
	7a		−0.52	8	4	8	64	157
	8a		0.42	4	8	128	256	>539
9a		0.72	2	4	8	128	>559	
Ciprofloxacin				0.06	<0.03	<0.03	0.25	

Bacterial reference strains: S. a – *Staphylococcus aureus* ATCC 9144, B. s – *Bacillus subtilis* 168, E. c – *Escherichia coli* ATCC 25922, and P. a – *Pseudomonas aeruginosa* ATCC 27853. All compounds were tested as di-TFA salts.

^a CLogP values were calculated for the respective non protonated cationic group (calculated with ChemBioDraw Ultra v19.0.0.1.28).

^b Values given as greater than correspond to the highest concentration (500 μM) tested in the RBC assay.

^c We have reported this compound previously having the following MIC values: S. a: 1 $\mu g/mL$, B. s: 2 $\mu g/mL$, E. c: 2 $\mu g/mL$, P. a: 4 $\mu g/mL$ [28].

^d Values were taken from Ref. [28].

or unsymmetrically **13(l,p)A** substituted primary amines in 34–76% yield (Scheme 2-IV). The Mitsunobu protocol was evaluated but discarded due to difficulties with purification of some compounds. Treatment of the primary amines with *N,N'*-di-Boc-1*H*-pyrazole-1-carboxamide and DIPEA, followed by TFA facilitated Boc removal and RP flash chromatography purification yielded the respective guanidines

13(c,e,h,i,j,l,p)G in 20–91% yield.

2.3. SAR analysis

All compounds were screened for antimicrobial activity against antibiotic susceptible Gram-positive and Gram-negative reference

Table 2Antimicrobial activity (MIC in $\mu\text{g/mL}$) against bacterial reference strains and haemolytic activity against human RBC (EC_{50} in $\mu\text{g/mL}$) for compounds in series 2.

Core structure	Comp. ID	$R^1 = R^2$	A/G	CLogP ^a	Antimicrobial activity				EC_{50} ^b
					S. a	B. s	E. c	P. a	
	10bA			2.53	256	64	>256	>256	>390
	10bG			2.53	8	16	128	>256	>432
	10cA			3.39	16	4	256	256	>469
	10cG			3.39	2	4	16	128	461
	10dA			3.87	16	8	32	64	>333
	10dG			3.87	2	2	4	16	143
	10eA			4.68	2	2	4	4	27
	10eG			4.68	4	4	4	8	36
	10fA			5.03	4	4	8	8	27
	10fG			5.03	4	4	4	8	32
	10gA			5.03	2	2	4	4	30
	10gG			5.03	2	1	4	4	30

Bacterial reference strains: S. a – *Staphylococcus aureus* ATCC 9144, B. s – *Bacillus subtilis* 168, E. c – *Escherichia coli* ATCC 25922, and P. a – *Pseudomonas aeruginosa* ATCC 27853. All compounds were tested as di-TFA salts.

^a CLogP values were calculated for the respective lipophilic side chains (calculated with ChemBioDraw Ultra v19.0.0.1.28).

^b Values given as *greater than* correspond to the highest concentration (500 μM) tested in the RBC assay.

strains (Tables 1–5). Haemolytic activity against human red blood cells (RBCs), expressed by the EC_{50} value, was used as a measurement of cytotoxicity. We have earlier reported compounds **1aA** and **1aG** [28], which here are used as reference compounds together with the known antibiotic ciprofloxacin as a positive control. The descriptors for amine derivatives (A) and guanidine derivatives (G) are omitted for derivatives with other cationic groups.

2.3.1. Compound series 1: Exploring the cationic head group (R^3)

First, we set out to investigate the influence of the effective charge of the cationic groups (Table 1, R^3 group and Fig. 2, blue space holders). Upon *N*-methylation the electron density at the nitrogen increases, as does its basicity, but the polarity decreases. Successive introduction of one (**6a**), two (**7a**) or three (**8a**) methyl groups had no noteworthy influence on the activity against the Gram-positive strains (MIC: 4–8 $\mu\text{g/mL}$), but the activity against the Gram-negative strains dropped considerably for compound **8a** (MIC: 128–256 $\mu\text{g/mL}$). It is suggested that, among other factors, the electrostatic interaction between these compounds and bacterial membrane plays an important role in the compound's activity [45]. Successive introduction of methyl groups lowers the effective charge of the amine head groups, thus reducing their interaction with the lower charge per area membrane of Gram-negative bacteria compared to Gram-positive strains [46]. Additionally, quaternary ammonium compounds (quats or QACs) are known for their impaired ability to cross the outer membrane of Gram-negative *Pseudomonas aeruginosa* (*P. aeruginosa*) [47]. Recent studies showed generally impaired uptake of compounds containing methylated primary amines in *E. coli* [31]. Despite that presumably lower uptake, secondary (**6a**) and tertiary amines (**7a**) were still active against *E. coli* (MIC: 8 $\mu\text{g/mL}$). By replacing the quaternary trimethylated ammonium (**8a**) with a pyridinium group (**9a**), the activity against the Gram-positive

strains improved (MIC: 2–4 $\mu\text{g/mL}$) and the activity against *E. coli* was restored (MIC: 8 $\mu\text{g/mL}$), probably due to increased accumulation [32]. Tertiary (**7a**), EC_{50} : 157 $\mu\text{g/mL}$ and quaternary amines (**8a** and **9a**; both EC_{50} : >500 $\mu\text{g/mL}$) displayed lower haemolytic activity compared to the primary (**1aA**, EC_{50} : 79 $\mu\text{g/mL}$) and secondary (**6a**, EC_{50} : 73 $\mu\text{g/mL}$) amines.

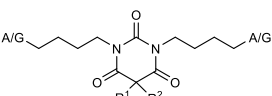
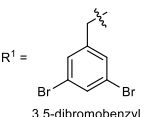
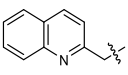
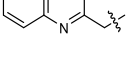
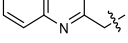
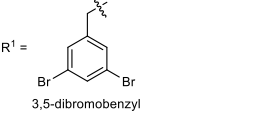
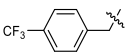
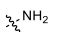
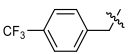
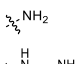
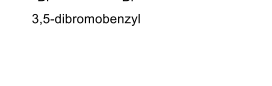
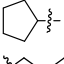
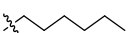
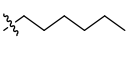
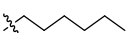

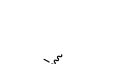
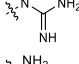
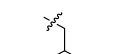
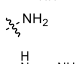

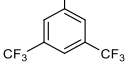
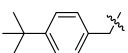
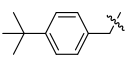
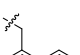

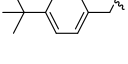
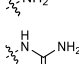
The quaternary ammonium compound **8a** exhibited narrow-spectrum antimicrobial activity against Gram-positive strains and was non-haemolytic. Compared to the above investigated head groups, the recently reported amine (**1aA**) and guanidine derivatives (**1aG**) appeared to be the most effective against the Gram-negative strains, thus rendering them suitable for broad-spectrum applications. The consecutively developed compounds were therefore synthesized with either amino or guanidino groups.

2.3.2. Compound series 2: Exploring new lipophilic side chains ($R^1 = R^2$)

In series 2, the influence of heterocyclic, aliphatic and highly brominated lipophilic side chains (Table 2, R^1/R^2 groups and Fig. 2, red space holders) on the biological activity was examined. Both side chains employed were identical.

The antimicrobial activity for the amine barbiturates **10(b-g)A** ranged from MIC: 2–256 $\mu\text{g/mL}$ and for the guanidine barbiturates **10(b-g)G** from MIC: 1–16 $\mu\text{g/mL}$ against the Gram-positive strains *Staphylococcus aureus* (*S. aureus*) and *Bacillus subtilis* (*B. subtilis*). Against the Gram-negative strains *E. coli* and *P. aeruginosa* both, the amine and guanidine derivatives, showed MIC values of 4 – >256 $\mu\text{g/mL}$. We included quinoline and 6-bromoquinoline as heterocyclic alternatives. The amine derivative **10bA** (R^1/R^2 = quinolin-2-ylmethyl) was neither antibacterial (MIC: ≥ 64 $\mu\text{g/mL}$) nor haemolytic, whereas the guanidine derivative **10bG** exhibited some activity against the Gram-positive strains (MIC: 8–16 $\mu\text{g/mL}$).

Table 3Antimicrobial activity (MIC in $\mu\text{g/mL}$) against bacterial reference strains and haemolytic activity against human RBC (EC_{50} in $\mu\text{g/mL}$) for compounds in series 3.

Core structure	Comp. ID	R^2	A/G	CLogP ^a	Antimicrobial activity				EC_{50} ^b
					S. a	B. s	E. c	P. a	
 $\text{R}^1 =$ 	11kA			3.45	32	8	128	256	>444
	11kG			3.45	2	4	32	32	450
	111A			3.95	16	8	32	64	342
	111G			3.95	2	4	2	16	161
	11mA			3.58	16	8	64	64	>407
	11nA			4.12	4	4	16	16	144
	11nG			4.12	2	4	4	8	58
	11oA			4.39	8	2	8	8	93
	11oG			4.39	2	2	2	4	36
	11pA			4.42	4	4	8	8	82
	11pG			4.42	2	2	2	4	39
	11qA			4.52	4	4	4	8	47
	11qG			4.52	1	4	4	8	58

Bacterial reference strains: S. a – *Staphylococcus aureus* ATCC 9144, B. s – *Bacillus subtilis* 168, E. c – *Escherichia coli* ATCC 25922, and P. a – *Pseudomonas aeruginosa* ATCC 27853. Guanidyl barbiturate **11mG** could not be obtained. All compounds were tested as di-TFA salts.

^a CLogP values were calculated for the respective lipophilic side chains and are presented as the average for the two substituents. (calculated with ChemBioDraw Ultra v19.0.0.1.28).

^b Values given as *greater than* correspond to the highest concentration (500 μM) tested in the RBC assay.

Upon inserting a bromine in the 6-position for **10cA** ($\text{R}^1/\text{R}^2 = (6\text{-bromoquinolin-2-yl)methyl}$) the CLogP rose considerably, and the amine derivative became active against the Gram-positive bacteria (MIC: 4–16 $\mu\text{g/mL}$). The respective guanidine **10cG** was found to be active against both the Gram-positive strains and *E. coli* (MIC: 2–16 $\mu\text{g/mL}$), while being nonhaemolytic. The bromine substituent seemed to be essential for good antimicrobial activity against Gram-positive strains and *E. coli*.

In the next step we replaced the aromatic side chains by alkyl chains as found in antimicrobial quats [48,49]. We decided to incorporate two hexyl chains, which mimic the single long alkyl chain commonly found in quats [50]. The amine derivative **10dA** ($\text{R}^1/\text{R}^2 = n\text{-hexyl}$) showed weak activity against all bacterial strains (MIC: 8–64 $\mu\text{g/mL}$), whereas the guanidine derivative **10dG** showed high antibacterial activity with MIC values of 2–4 $\mu\text{g/mL}$ against all strains except for *P. aeruginosa*. Haemolysis was still moderate, with EC_{50} : 143 $\mu\text{g/mL}$. Interestingly, the shorter hexyl chains perform just as good as the longer alkyl chains in quats [48], suggesting that the overall hydrophobic bulk is more important than the actual chain length.

Compounds **10e** ($\text{R}^1/\text{R}^2 = (4\text{-bromonaphthalen-1-yl)methyl}$) were prepared based on the previously reported (4-fluoronaphthalen-1-yl) methyl barbituric acid [28]. Introduction of electron withdrawing fluorine into molecules is known to hamper *in vivo* oxidation of aromatic side chains during Phase I metabolism [51,52]. Replacing the fluorine for a bromine increases the hydrophobic bulk, while having similar electronic effects [53]. Surprisingly, the amine derivative **10eA** was equally potent as the guanidine **10eG** with MIC values of 2–8 $\mu\text{g/mL}$ against all reference strains. However, both, **10eA** and **10eG**, were also highly haemolytic (EC_{50} : 27–36 $\mu\text{g/mL}$).

Previously, we have found bromo substituents on the phenyl ring having a positive effect on the biological activity, with 3,5-dibromophenyl providing the highest activity [26]. We therefore prepared derivatives **10fA** and **10fG** ($\text{R}^1/\text{R}^2 = 2,4,5\text{-tribromobenzyl}$) and **10gA** and **10gG** ($\text{R}^1/\text{R}^2 = 2,4,6\text{-tribromobenzyl}$) being at the far end of the hydrophobicity scale. They all displayed potent antibacterial activity, with MIC values ≤ 8 $\mu\text{g/mL}$ against all strains. However, haemolytic activity also increased for all these compounds (EC_{50} : 27–32 $\mu\text{g/mL}$). The positioning of the bromines on the phenyl ring had a minor influence on antibacterial activity, with **10gA** and **10gG** being most potent.

In summary, halogenated heterocycles are promising side chains for narrow-spectrum application. The hydrophobicity of the C-5 substituents had the greatest influence, while the structure being secondary. When exceeding $\text{CLogP} \approx 4.50$, the structures mostly became too haemolytic to be of interest for further studies.

2.3.3. Compound series 3: Exploring mixed lipophilic groups ($\text{R}^1 \neq \text{R}^2$)

A series of compounds containing two different side chains were prepared to tune lipophilicity and side chain structure with respect to antimicrobial activity and haemolytic activity. We intended to pair the potent 3,5-dibromobenzyl side chain (R^1) with side chains (R^2) of different varying lipophilicity (Table 3; R^2 group; Fig. 2, red space holders).

First, we chose to incorporate previously documented non potent side chains (see series 2 and previously reported [26,28]) in compounds **11k** ($\text{R}^2 = \text{quinolin-2-ylmethyl}$) and **11l** ($\text{R}^2 = 4\text{-(trifluoromethyl)benzyl}$). The amine derivatives **11kA** and **111A** displayed weak activity, mainly against *B. subtilis* (MIC: 8 $\mu\text{g/mL}$) but can be considered non-haemolytic. The guanidine derivatives **11kG** and **111G** were still

Table 4Antimicrobial activity (MIC in $\mu\text{g/mL}$) against bacterial reference strains and haemolytic activity against human RBC (EC_{50} in $\mu\text{g/mL}$) for compounds in series 4.

Core structure	Comp. ID	X	A/G	CLogP ^a	Antimicrobial activity				EC ₅₀
					S. a	B. s	E. c	P. a	
	12aA			1.75	4	4	4	8	39
	12aG			1.75	2	2	4	16	164
	13aA			2.28	4	4	8	8	99
	13aG			2.28	2	2	4	8	187
	14aA			3.34	4	4	8	8	24
	14aG			3.34	4	4	4	8	29 ^b
	15aA			3.87	4	4	4	16	30
	15aG			3.87	4	4	4	32	57 ^b
	16aA			2.24	8	4	4	8	50
	16aG			2.24	2	2	4	8	75
	17aA			2.24	4	4	4	8	93
	17aG			2.24	2	4	4	8	62
	18aA			3.35	4	4	4	8	15
	18aG			3.35	2	1	4	4	30
	19aA			3.35	2	2	2	4	16

Bacterial reference strains: S. a – *Staphylococcus aureus* ATCC 9144, B. s – *Bacillus subtilis* 168, E. c – *Escherichia coli* ATCC 25922, and P. a – *Pseudomonas aeruginosa* ATCC 27853. All compounds were tested as di-TFA salts. Compound **19aG** was not obtained in satisfying purity.

^a CLogP values were calculated for the respective hydrocarbon linkers (calculated with ChemBioDraw Ultra v19.0.0.1.28).

^b Precipitation in the RBC assay observed.

almost non-haemolytic (EC_{50} : down to 161 $\mu\text{g/mL}$) and displayed potent activity against the Gram-positive strains (MIC: 2–4 $\mu\text{g/mL}$).

The derivative **11iG** showed additionally good activity against the Gram-negative *E. coli* (MIC: 4 $\mu\text{g/mL}$). The superior performance of **11iG** over **11kG** may be attributed to the higher average CLogP value of the lipophilic side chain of **11iG**. The polar nitrogen atom in the quinolinyl side chain (**11iG**) might also reduce the compounds' activity.

Next, we tested two hydrocarbon analogues **11m** (R^2 = cyclopentyl) and **11n** (R^2 = *n*-hexyl), with comparable average hydrophobicity to **11k** and **11l**, respectively. Compound **11mA** was potent against both Gram-positive strains and non-haemolytic. The amine derivative **11nA** was mainly acting against the Gram-positive strains (MIC: 4 $\mu\text{g/mL}$) but showed 3-fold higher haemolytic activity compared to **11IA**. The guanyl derivative **11nG** exhibited potent antibacterial activity, with MIC-values of 2–8 $\mu\text{g/mL}$ against all strains tested. Even though its average CLogP was only marginally higher than **11iG**, its haemolytic activity was pronouncedly higher (EC_{50} : 58 $\mu\text{g/mL}$). The compounds **11m** and **11n** indicated that a combination of an aromatic and a hydrocarbon lipophilic side chain leads to higher haemolytic activity, compared to two aromatic side chains.

To study the influence of the structure of the lipophilic side chains we prepared structurally different, but of similar lipophilicity, compounds **11o** (R^2 = 3,5-bis(trifluoromethyl)benzyl), **11p** (R^2 = 4-(*tert*-butyl)benzyl), and **11q** (R^2 = (4-bromonaphthalen-1-yl)methyl). All their amine derivatives displayed low MIC values of 2–8 $\mu\text{g/mL}$ against all reference strains and **11oA** was least haemolytic (EC_{50} : 93 $\mu\text{g/mL}$).

Upon guanylation, a further improvement in antimicrobial activity was achieved, but haemolytic activity was also increased. Thus, **11oG** and **11pG** became twice as potent and haemolytic (EC_{50} : 36–39 $\mu\text{g/mL}$), rendering them unfavorable for systemic *in vivo* treatment. The bromonaphthyl containing **11qG** became more potent against *S. aureus* (MIC: 1 $\mu\text{g/mL}$), yet haemolytic activity (EC_{50} : 58 $\mu\text{g/mL}$) was still unfavorably high. No clear trend for the antimicrobial activity could be deduced, based on the structure of the lipophilic side chains.

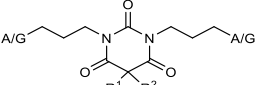
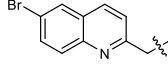
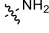
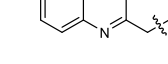
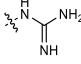
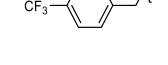
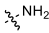

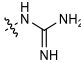
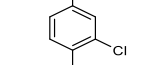
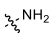
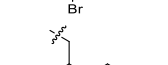
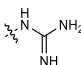
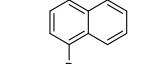
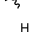
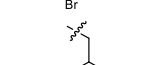
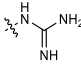
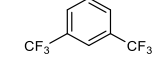
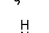
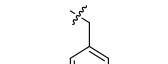
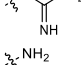
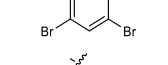
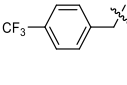
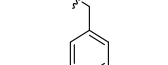
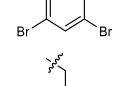
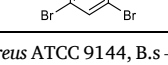
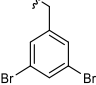

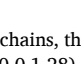
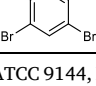
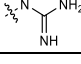
Taken all together, **11kG** displayed promising narrow-spectrum activity against Gram-positive strains and absence of haemolytic activity. Compounds **11oG** and **11pG** are highly potent derivatives but displayed high haemolytic activity.

2.3.4. Compound series 4: Exploring the hydrocarbon linker chain (X)

We incorporated various linear and cyclic hydrocarbon linkers (Tables 4 and X group; Fig. 2, green space holder) between the central scaffold and the cationic residue. 3,5-Dibromobenzyl was kept fixed as the lipophilic side chain and the previously reported compounds **1aA** and **1aG** (both X = *n*-butyl) served as reference substances for comparison. Shortening or elongating the alkyl chains to 2, 3, 5 or 6 methylene groups (**12aA–15aA**) led to no significant change in antibacterial activity (MIC: 4–16 $\mu\text{g/mL}$ against all strains). The haemolytic activity increased slightly compared to **1aA** (X = *n*-butyl), except for **13aA** (X = *n*-propyl), which became slightly less haemolytic. So far, guanidine derivatives tended to have a higher haemolytic activity (*vide supra*) compared to amine derivatives. In contrast, **13aG** (X = *n*-propyl) and

Table 5

Antimicrobial activity (MIC in $\mu\text{g/mL}$) against bacterial reference strains and haemolytic activity against human RBC (EC_{50} in $\mu\text{g/mL}$) for compounds in series 5.

Core structure	Comp ID	R ¹	R ²	A/G	CLogP ^a	Antimicrobial activity				EC ₅₀ ^b	
						S. a	B. s	E. c	P. a		
	13cA		R ² = R ¹		3.39	32	8	64	256	>455	
	13cG				3.39	8	4	64	>128	>497	
	13hA		R ² = R ¹		3.87	64	16	64	128	>393	
	13hG				3.87	8	4	128	256	>435	
	13iA		R ² = R ¹		4.08	8	4	8	16	323	
	13iG				4.08	2	2	8	32	348	
	13eA		R ² = R ¹		4.68	2	2	4	4	23	
	13eG				4.68	2	2	4	8	61	
	13jA		R ² = R ¹		5.03	8	4	8	8	176	
	13jG				5.03	4	2	8	16	445	
	13lA					3.95	32	8	16	32	>438
	13lG					3.95	4	4	16	64	>480
	13pA					4.42	4	2	8	8	47
	13pG					4.42	1	1	2	16	169

Bacterial reference strains: S. a – *Staphylococcus aureus* ATCC 9144, B. s – *Bacillus subtilis* 168, E. c – *Escherichia coli* ATCC 25922, and P. a – *Pseudomonas aeruginosa* ATCC 27853. All compounds were tested as di-TFA salts.

^a CLogP values were calculated for the respective lipophilic side chains. For non-identical side chains, the value stated is the average of both individual side chains. Values were calculated for substituted benzyl groups (calculated with ChemBioDraw Ultra v19.0.0.1.28).

^b Values given as *greater than* correspond to the highest concentration (500 μM) tested in the RBC assay.

12aG (X = ethyl) were observed to exhibit 2-fold and 4-fold decreased haemolytic activity, respectively, compared to their amine counterparts. The activity against the Gram-positive strains was slightly improved, whereas the potencies against the Gram-negative *P. aeruginosa* were retained or a little diminished. The derivatives 14aA and 14aG (X = *n*-pentyl) displayed virtually the same MIC and EC₅₀ values, whereas 15aG (X = *n*-hexyl) was less potent against *P. aeruginosa* (MIC: 32 $\mu\text{g/mL}$) compared to 15aA (X = *n*-hexyl) (MIC: 16 $\mu\text{g/mL}$). Both guanylated compounds were less potent than the previously investigated derivative 1aG (X = *n*-butyl) and their haemolytic levels were comparably high (EC₅₀: 29–57 $\mu\text{g/mL}$). Compounds 14aG (X = *n*-pentyl) and 15aG (X = *n*-hexyl) led also to precipitation in the RBC assay upon sample preparation, possibly due to their higher overall hydrophobicity, demonstrating an unfavorable solubility profile.

To investigate if the conformational freedom of the linker influenced the compounds potency, 1,3-cyclobutyl and 1,4-cyclohexyl were used as surrogates for the *n*-propyl and *n*-butyl chains, taking advantage of their restricted spatial arrangement. Compounds 16aA (X = *cis*-1,3-cyclobutyl) and 17aA (X = *trans*-1,3-cyclobutyl) displayed the same MIC values (4–8 $\mu\text{g/mL}$) as 13aA (X = *n*-propyl) against all strains, but 16aA (*cis*) was almost twice as haemolytic as 13aA (X = *n*-propyl) and 17aA (*trans*). Their guanylated counterparts 16aG (*cis*) and 17aG (*trans*), were more potent against the Gram-positive strains, but no change in MIC was observed against the Gram-negative strains. Both derivatives exhibited considerably higher haemolytic activity compared to 13aG (X = *n*-propyl).

While being equally haemolytic (EC₅₀: 15 $\mu\text{g/mL}$) and 5-times more haemolytic than 1aA (X = *n*-butyl), 19aA (X = *trans*-1,4-cyclohexyl) was twice as potent as 18aA (X = *cis*-1,4-cyclohexyl). The guanidine derivative 18aG (*cis*) was highly potent (MIC: 1–4 $\mu\text{g/mL}$) against all bacterial strains, but its haemolytic activity was also too high to be of therapeutic value for systemic application. Of note, the guanylated derivative (18aG) was nevertheless less haemolytic than the amine derivative (18aA).

In summary, compounds with rigid cyclic linkers showed similar or slightly higher potency compared to their linear analogues, but they tended to be more haemolytic. Furthermore, compounds with pentyl and hexyl linkers showed furthermore decreased water solubility. The amine derivatives having ethyl, *n*-propyl or *n*-butyl linkers displayed similar antibacterial bioactivity profiles, whereas the equivalent guanidine derivatives displayed descending antimicrobial activity as follows: *n*-butyl > *n*-propyl > ethyl. The best balance between high antimicrobial activity and low haemolytic activity was presented by compounds having *n*-propyl hydrocarbon linker chains.

2.3.5. Compound series 5: Investigating compounds with a *n*-propyl hydrocarbon linker

In series 5 (Table 5), we studied the effect of the *n*-propyl linker more closely due to the promising balance between high antimicrobial activity and low haemolytic activity seen in series 4. We selected the lipophilic side chains (R¹/R²) based on our previous findings. We reasoned that compounds 13c, 13h and 13l would mainly act against

Gram-positive strains, whereas compounds **13e**, **13i**, **13j** and **13p** should provide a higher broad-spectrum activity. Amines **13cA** ($R^1/R^2 = (6\text{-bromoquinolin-2-yl)methyl}$) and **13hA** ($R^1/R^2 = 4\text{-}(trifluoromethyl)\text{benzyl}$) displayed generally low antibacterial activity against all strains (MIC: 8–256 $\mu\text{g/mL}$). However, the guanyl equivalents **13cG** and **13hG** exhibited fair activity and selectivity for Gram-positive strains (MIC: 4–8 $\mu\text{g/mL}$) and weak activity towards Gram-negative strain (MIC: ≥ 64 $\mu\text{g/mL}$). None of the four compounds was haemolytic.

Compound **13iA** ($R^1/R^2 = 4\text{-bromo-3-chlorobenzyl}$) displayed good activity against all strains (MIC: 4–8 $\mu\text{g/mL}$) except for the Gram-negative *P. aeruginosa* (MIC: 16 $\mu\text{g/mL}$). The guanyl derivative **13iG** displayed further improved activity against the Gram-positive strains (MIC: 2 $\mu\text{g/mL}$), but the activity against *P. aeruginosa* was lost. Noteworthy, the amine **13iA** and guanidine **13iG** derivatives were non-haemolytic (EC_{50} : >300 $\mu\text{g/mL}$), despite the relatively high CLogP values of their lipophilic side chains.

Derivatives **13eA** and **13eG** contained the bulky bromo-naphthyl ($R^1/R^2 = (4\text{-bromonaphthalen-1-yl)methyl}$) group. The amine derivative **13eA** was highly potent (MIC: 2–4 $\mu\text{g/mL}$) against all strains, but too haemolytic to be of practical use (EC_{50} : 23 $\mu\text{g/mL}$). Upon guanylation, **13eG** still had good activity against all strains (MIC: 2–8 $\mu\text{g/mL}$) and an almost three-fold decrease in haemolytic activity (EC_{50} : 61 $\mu\text{g/mL}$) was observed. The relatively high haemolytic activity was still unfavorable, but the positive effect of exchanging *n*-butyl linkers (**10eG**) for *n*-propyl linkers (**13eG**) was well demonstrated.

The amine derivative **13jA**, featuring 3,5-bis(trifluoromethyl)benzyl side chains, was potent against all strains (MIC: 4–8 $\mu\text{g/mL}$) and displayed low haemolytic activity (EC_{50} : 176 $\mu\text{g/mL}$). The guanyl analogue **13jG** was twice as potent against the Gram-positive strains, while the activity against *P. aeruginosa* was reduced (MIC: 16 $\mu\text{g/mL}$). Pleasingly, the guanylation rendered the compound non-haemolytic.

The unsymmetrically C-5 substituted amine **13lA** ($R^1 = 3,5\text{-dibromobenzyl}$, $R^2 = 4\text{-}(trifluoromethyl)\text{benzyl}$) displayed acceptable activity only against *B. subtilis* (MIC: 8 $\mu\text{g/mL}$). The guanyl derivative **13lG** exhibited good activity against both Gram-positive strains (MIC: 4 $\mu\text{g/mL}$), but its intermediate activity against Gram-negative *E. coli* (MIC: 16 $\mu\text{g/mL}$) limits its narrow-spectrum application against Gram-positive bacteria.

The unsymmetrically substituted amine **13pA** ($R^1 = 3,5\text{-dibromobenzyl}$, $R^2 = 4\text{-}(tert\text{-butyl})\text{benzyl}$) was potent against all strains tested (MIC: 2–8 $\mu\text{g/mL}$) but was quite haemolytic (EC_{50} : 47 $\mu\text{g/mL}$). The guanyl derivative **13pG** became more potent against all strains but *P. aeruginosa* (MIC: 16 $\mu\text{g/mL}$), accompanied by an almost 4-fold decrease in haemolytic activity (EC_{50} : 169 $\mu\text{g/mL}$), rendering it a very promising candidate for further studies.

Using *n*-propyl linkers clearly had a positive effect and led to development of the potent derivatives **13iA**, **13jA**, **13jG**, **13lG** and **13pG** with broad-spectrum activity. All five derivatives displayed low haemolytic activity, making them promising candidates for further evaluation.

2.3.6. Trends in haemolytic activity

When examining the haemolytic activity of our compounds we saw a pronounced difference between compounds having *n*-propyl and *n*-butyl linkers. The core findings are presented in the following paragraph and a more detailed section on how the structures were compared can be found in chapter 1 of the Supporting Information.

For our comparison, we selected 24 compounds and assorted them into four scaffold groups (Fig. S1) based on the combination of linkers and cationic head groups. Compounds with (i) *n*-propyl linkers and amine groups were placed in group 3CA, (ii) *n*-propyl linkers and guanidyl groups in group 3CG, (iii) *n*-butyl linkers and amine groups in group 4CA and (iv) *n*-butyl linkers and guanidyl groups in group 4CG. Each scaffold group contained compounds with the following side chain combinations: **a** (3,5-dibromobenzyl), **e** ((4-bromonaphthalen-1-yl)methyl), **i** (4-bromo-3-chlorobenzyl), **j** (3,5-bis(trifluoromethyl)benzyl),

l ($R^2 = 4\text{-}(trifluoromethyl)\text{benzyl}$) and **p** (4-(*tert*-butyl)benzyl). To represent the trends, we have looked at the difference in EC_{50} values between 3CG – 3CA and 4CG – 4CA (Fig. S2) as well as 3CA – 4CA and 4CG – 3CG (Fig. S3).

First, we compared guanidyl- and amine-containing compounds with the same linkers and lipophilic side chains. For compounds with *n*-butyl linkers (4CG – 4CA), all guanidyl containing compounds were more haemolytic than their amine counterparts except for when the (4-bromonaphthalen-1-yl)methyl (**e**) was present. Comparing *n*-propyl containing derivatives (3CG – 3CA), we observed the reversed trend. The guanidyl derivatives were equally to pronouncedly less haemolytic than their amine counterparts. The difference in EC_{50} values ranged from 0 $\mu\text{g/mL}$ for side chain combination **l** to 269 $\mu\text{g/mL}$ for side chain combination **j**.

Next, we compared the *n*-butyl with *n*-propyl linkers in the presence of amine groups (3CA – 4CA). For side chain combinations **a**, **e**, **j** and **p** the compounds were of comparable haemolytic activity regardless of the linker length. Only for side chain combinations **i** and **l** the derivatives with *n*-propyl linkers (3CA) were less haemolytic by 151 and 158 $\mu\text{g/mL}$, respectively, compared to their *n*-butyl counterparts (4CA). The difference between *n*-butyl and *n*-propyl linkers was most eminent in the presence of guanidyl groups (4CG – 3CG). All compounds having *n*-propyl linkers (3CG) were less haemolytic than compounds with *n*-butyl linkers (4CG). The difference ranged from 25 $\mu\text{g/mL}$ for side chain combination **e** to an impressive 347 $\mu\text{g/mL}$ for side chain combination **j**.

This comparison clearly shows that *n*-propyl linkers not only led to derivatives with good broad-spectrum activity, but also low haemolytic activity. Despite the often noteworthy difference in EC_{50} values for the two linkers, no obvious SAR could be delineated.

2.3.7. Summary of SAR analysis

The general trends of our SAR analysis are summarized in Fig. 3. When assessing the potency of the lipophilic side chains and the hydrocarbon linkers, amine and guanidine derivatives were not distinguished, as they generally follow the same trends.

We found that the antimicrobial activity decreased along the line of *n*-butyl > *n*-propyl > ethyl and haemolytic activity increased as follows: *n*-propyl < ethyl < *n*-butyl. The cyclic hydrocarbons, *n*-pentyl and *n*-hexyl displayed varying MIC values, but where all too haemolytic to be of any practical use and were therefore excluded from the list. Guanyl compounds with *n*-butyl linkers were more haemolytic than their amine counterparts. As mentioned before, for ethyl and *n*-propyl linkers this

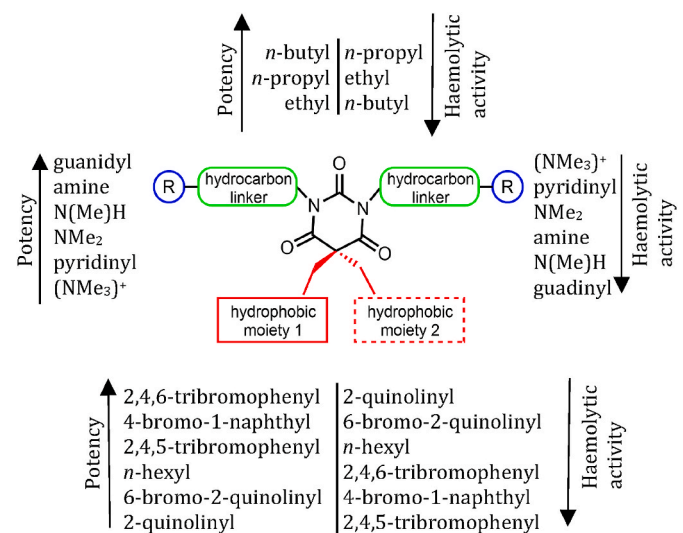


Fig. 3. Overview over the general trends observed during the SAR investigation. The trends for haemolytic activity were assessed for the average between the respective amines and guanidines.

trend was reversed. Based on this, *n*-propyl seemed to be the best compromise to achieve high antimicrobial activity and moderate haemolytic activity.

In line with our previous findings, the compounds potency and haemolytic activity increased with higher CLogP values of the lipophilic side chains for both, amines and guanidines. Bromines proved to be a good modulator of the hydrophobicity of aryl groups. The structure of the side chains seemed thereby to be secondary. The most potent compounds proved to be too haemolytic for future therapeutic considerations. By combining two lipophilic side chains of different structure and hydrophobicity (**11kG** and **11IG**), antimicrobial potency and haemolytic activity of the compounds could be fine-tuned.

To achieve good broad-spectrum activity, amine or guanidine groups proved to be necessary. Methylated primary amines showed reduced activity against Gram-negative *P. aeruginosa* alongside reduced haemolytic activity. The least haemolytic cationic groups were the quaternary ammonium compounds in **8a** and **9a**. Due to its lack of haemolytic activity and high activity against Gram-positive bacterial strains, **8a** could prove valuable for narrow-spectrum applications against Gram-positive bacteria.

2.4. Selectivity index

A common measurement for the efficiency of antimicrobial agents is the selectivity index (SI) given by the ratio EC₅₀/MIC values (for all SI values see Table S1). Our efforts led to promising candidates for narrow as well as broad-spectrum applications. We have grouped them into three groups (Table 6) based on their activity and SI against Gram-positive strains (entries 1–4), Gram-positive strains and *E. coli* (entries 5–7) and all strains tested (entries 8–11), respectively. Compounds were considered active if the MIC values were ≤16 µg/mL.

The first group, **8a**, **11kG**, **13cG** and **13hG** (Table 6, entries 1–4), comprised compounds that had a SI ≥ 54 for the Gram-positive strains, while showing no activity against Gram-negative strains and human red blood cells. These properties make them ideal candidates for narrow-spectrum application against Gram-positive bacteria.

Compounds in the second group had SI ≥ 40 (Table 6, entries 5–7) against the Gram-positive strains and the Gram-negative *E. coli* and a medium SI (<20) against Gram-negative *P. aeruginosa*. Of the three compounds **9**, **11IG** and **13pG**, only pyridinyl derivative **9** (entry 5) did not show measurable haemolytic activity. But despite having moderate EC₅₀ values (161 and 169 µg/mL), guanyl derivatives **11IG** and **13pG**

Table 6

Selectivity index (SI) of the most promising wide and narrow-spectrum antimicrobials. EC₅₀ values are given in [µg/mL].

Entry	Comp. ID	SI (EC ₅₀ /MIC) ^a				EC ₅₀ ^b
		S. a	B. s	E. c	P. a	
1	8a	>135	>67	–	–	>539
2	11kG	225	113	–	–	450
3	13cG	>62	>124	–	–	>497
4	13hG	>54	>109	–	–	>435
5	9a	>280	>140	>70	–	>559
6	11IG	81	40	81	10	161
7	13pG	169	169	85	11	169
8	13aG	93	93	47	23	187
9	13jA	23	46	23	23	176
10	13jG	111	222	56	28	445
11	13iA	40	81	40	20	323
12	1aA	20	40	20	10	79
13	1aG	31	31	31	8	62

Bacterial reference strains: S. a – *Staphylococcus aureus* ATCC 9144, B. s – *Bacillus subtilis* 168, E. c – *Escherichia coli* ATCC 25922, and P. a – *Pseudomonas aeruginosa* ATCC 27853.

^a No SI was calculated if the MIC was >16 µg/mL.

^b Values given as *greater than* correspond to the highest concentration (500 µM) tested in the RBC assay.

had a high SI.

The third group comprises molecules with a SI ≥ 20 (Table 6, entries 8–11) against all four strains. Compounds **13aG** and **13jA** (entries 8–9) displayed a good overall SI and had also good activity against the Gram-negative *P. aeruginosa* (MIC: 8 µg/mL). Compounds **13jG** and **13iA** (entries 10–11) were mildly potent against *P. aeruginosa* (MIC: 16 µg/mL), but due to their low haemolytic activity they still display promising SI values. Their absence of cytotoxicity makes them promising candidates, despite their mild activity against Gram-negative *P. aeruginosa*, keeping in mind that most naturally occurring AMPs display low activity against this Gram-negative strain as well [17]. Additionally, group 3 compounds generally matched or outperformed our reference compounds **1aA** and **1aG** (entries 12–13).

2.5. Effect of the counterion on solubility and activity

The counterion of acidic and basic drugs is known to greatly influence their overall physicochemical properties such as solubility, membrane permeability and stability [54,55]. From the long list of physiological anions for basic active pharmaceutical ingredients (APIs), hydrochloride salts are predominant [55] and known to improve water solubility [56].

We found that the water solubility of the TFA salts decreased noticeably when the CLogP values of the lipophilic side chains rose beyond 4. To study if we could counteract this trend, we converted selected compounds to HCl salts. Additionally, we wanted to investigate if the counterion affected the biological activity. Table 7 summarizes the re-evaluated MIC and EC₅₀ values of selected compounds as hydrochloride salts. Water solubility was assessed qualitatively by setting the threshold at 1 mg/mL. Entries 1–3 show that previously not soluble (–) TFA salts became soluble (+). Compound **13iG** (entry 4) and several others (data not shown) remained poorly soluble in water, especially if several bromine substituents were present in the lipophilic side chain.

Hydrochloride salts of the amine derivatives **13iA** and **13jA** exhibited no change in their MIC values and showed only slightly differing EC₅₀ values (entries 1–2). No clear trend could be observed whether hydrochloride salts tended to be more or less haemolytic than TFA salts. Surprisingly, the HCl salts of guanyl derivatives **13iG** and **13jG** displayed improved MIC values against *S. aureus* (Entries 3–4), while the activity against *E. coli* remained unchanged. Compound **13jG** was the only HCl salt being considerably more haemolytic than its TFA counterpart (Entry 3), for yet undetermined reasons. The deceptively higher haemolytic activity of derivatives **13iA** and **13iG** as HCl salts (Entry 2 and 4) can be attributed to the lower molecular weight of the HCl salts.

2.6. Mode of action studies

Luciferase-based biosensor assays (viability and membrane integrity)

Table 7

MIC and EC₅₀ values in µg/mL of selected di-TFA (first value) and dihydrochloride (HCl, second value) salts. Improved values are highlighted in green.

Entry	Code	MIC [µg/mL] ^a		EC ₅₀ [µg/mL]	Solubility ^b
		S. a	E. c		
1	13jA	8/8	8/8	176/224	–/+
2	13iA	8/8	8/8	323/271 ^c	–/+
3	13jG	4/2	8/8	445/118	–/+
4	13iG	2/0.5	8/8	348/291 ^d	–/–

^a Bacterial reference strains: S. a – *Staphylococcus aureus* ATCC 9144 and E. c – *Escherichia coli* ATCC 25922.

^b If solubility in pure water is equal or greater than 1 mg/mL it is denoted with (+), if lower (–).

^c EC₅₀ = 368/375 µM (TFA/HCl).

^d EC₅₀ = 362/362 µM (TFA/HCl).

were performed to explore the mode of action of promising compounds on *B. subtilis* 168 and *E. coli* K12 [57]. The biosensor-based viability assay measures bacterial viability as light production through recombinantly expressed bacterial luciferase originating from the *Photobacterium luminescens lux* operon. The addition of external substrates does not affect the production of light by the bacterial *lux* operon. The bacterium itself provides the pool of reduced flavin mononucleotide (FMNH₂) and long-chain aliphatic aldehydes, which are the substrates responsible for light production. Bacterial luciferase is an excellent real-time sensor for bacterial viability, as NADH, NADPH, and ATP are necessary to constantly top up the substrates' pool.

The biosensor-based membrane integrity assay depends on the luciferase (*lucGR* gene) originating from the luminous click beetle *Pyrophorus plagiophthalmus*. In contrast to bacterial luciferase, the light reaction of *lucGR* is stringently reliant on the substrate D-luciferin, which is added externally. D-luciferin is inadequately crossing intact biological membranes at neutral pH. After the addition of antimicrobial substances, the uptake is explored to determine if the membrane becomes permeable to the substrate D-luciferin. An increase in light production occurs when D-luciferin enters (increased influx) through a compromised membrane. Light production peaks rapidly if membrane integrity is compromised and, thereafter, usually decreases while the ATP from dying cells is consumed.

Based on structural modifications, MIC values, haemolytic activity, and selectivity index, 17 compounds were selected for mode of action studies against *B. subtilis* 168 (see Supporting Information, Table S2) as they were mainly potent against Gram-positive bacteria. Furthermore, based on their broad-spectrum activity, 14 additional compounds were tested against both, the Gram-positive *B. subtilis* 168 and the Gram-negative *E. coli* K12 biosensor strain (see the Supporting Information, Tables S2 and S3). In general, most of the compounds tested affected viability and showed strong membrane disrupting activity against both bacterial strains. However, some of the compounds showed a more pronounced effect on viability and a faster membranolytic effect against

B. subtilis compared to *E. coli*. For most compounds, both viability and membrane integrity were affected when the concentration of the compounds was higher than the MIC value. Additionally, increasing concentrations affected viability and membranolytic activity in increasing rates, indicating a concentration-dependent killing effect. We could not determine any relationship between structure/activity and the mode of action profiles.

We selected the broad-spectrum barbiturate **111G** to exemplify the results of the viability and membrane integrity assay in detail (Fig. 4 and Fig. 5). Barbiturate **111G** clearly affected the viability of *B. subtilis* (Fig. 4A, left). The membrane integrity assay was performed on the *B. subtilis* biosensor strain to confirm that the rapid decrease in bacterial viability was caused by membrane damage. Derivative **111G** showed a membrane-related mode of action as light emission decreased rapidly in a dose-dependent manner (Fig. 4B, left), similar to chlorhexidine (CHX) (Fig. 4B, right). The reference control CHX is a bactericidal agent recognized for its cell wall and membrane disruptive properties [58], with MIC values of 1.5 µg/mL against both, *B. subtilis* 168 and *E. coli* K12. The disruptive membrane effect of barbiturate **111G** on *B. subtilis* was shown at a concentration as low as 6.4 µg/mL, which is approximately 1.6 times higher than its MIC (4 µg/mL) (Fig. 4B, left). The lowest concentration (3.2 µg/mL), which is slightly lower than its MIC value, showed a limited membrane disruption effect and the peak emission did not decline during the assay period. The bacterial concentration for these experiments was approximately 100 times higher than the concentration used in the MIC assay, which could explain why slightly higher concentrations of barbiturate **111G** were needed to affect the viability and membrane integrity.

When it comes to the effects of barbiturate **111G** on the viability and membrane integrity in the Gram-negative *E. coli*, the picture is somewhat different from that of the Gram-positive *B. subtilis*. The broad-spectrum derivative **111G** affected the viability of the *E. coli* strain and showed a concentration-dependent killing effect like CHX (Fig. 5A). Although **111G** affected the viability, a much less prominent inner

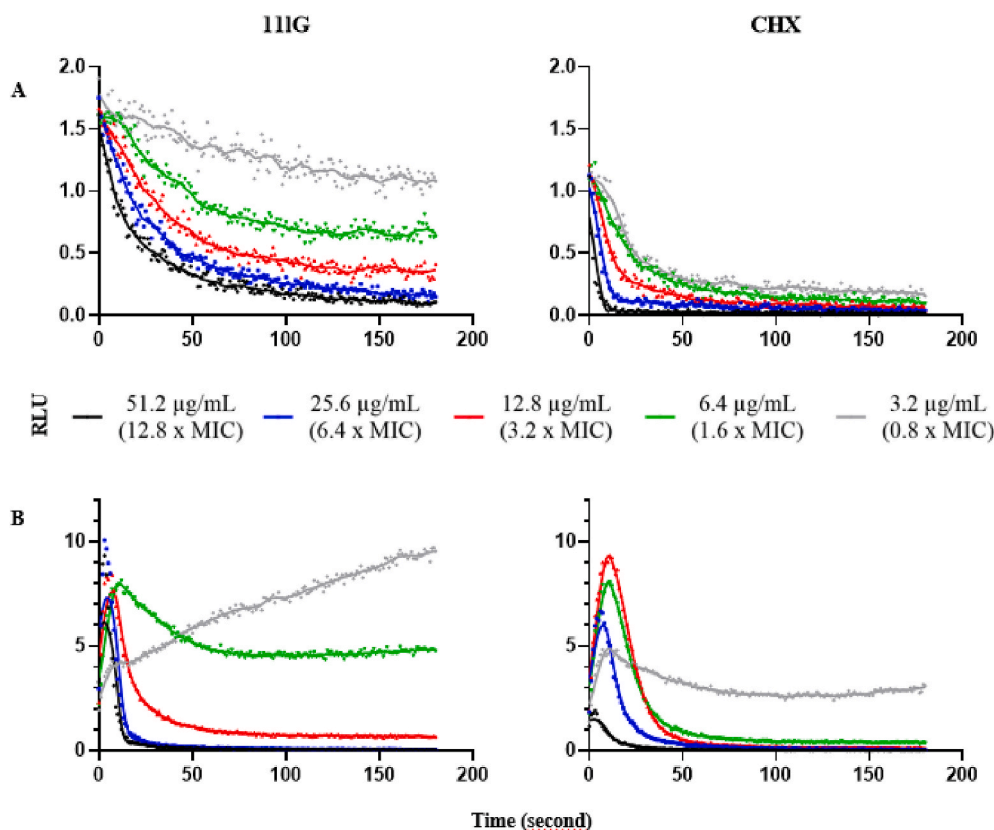


Fig. 4. The effects of **111G** (broad-spectrum) and CHX (positive control) on the kinetics of (A) viability and (B) membrane integrity in *B. subtilis* 168. Normalized light emission (normalized with a negative, untreated water control) is plotted as relative light units (RLU) over time (seconds). Light emission was measured each second for 180 s after adding the bacterial cell suspension (with 1 mM D-luciferin for the membrane integrity assay) to the analytes in separate wells. The multiples of the MIC values given in parentheses refers only to compound **111G**. The figure shows a representative data set from at least three independent experiments.

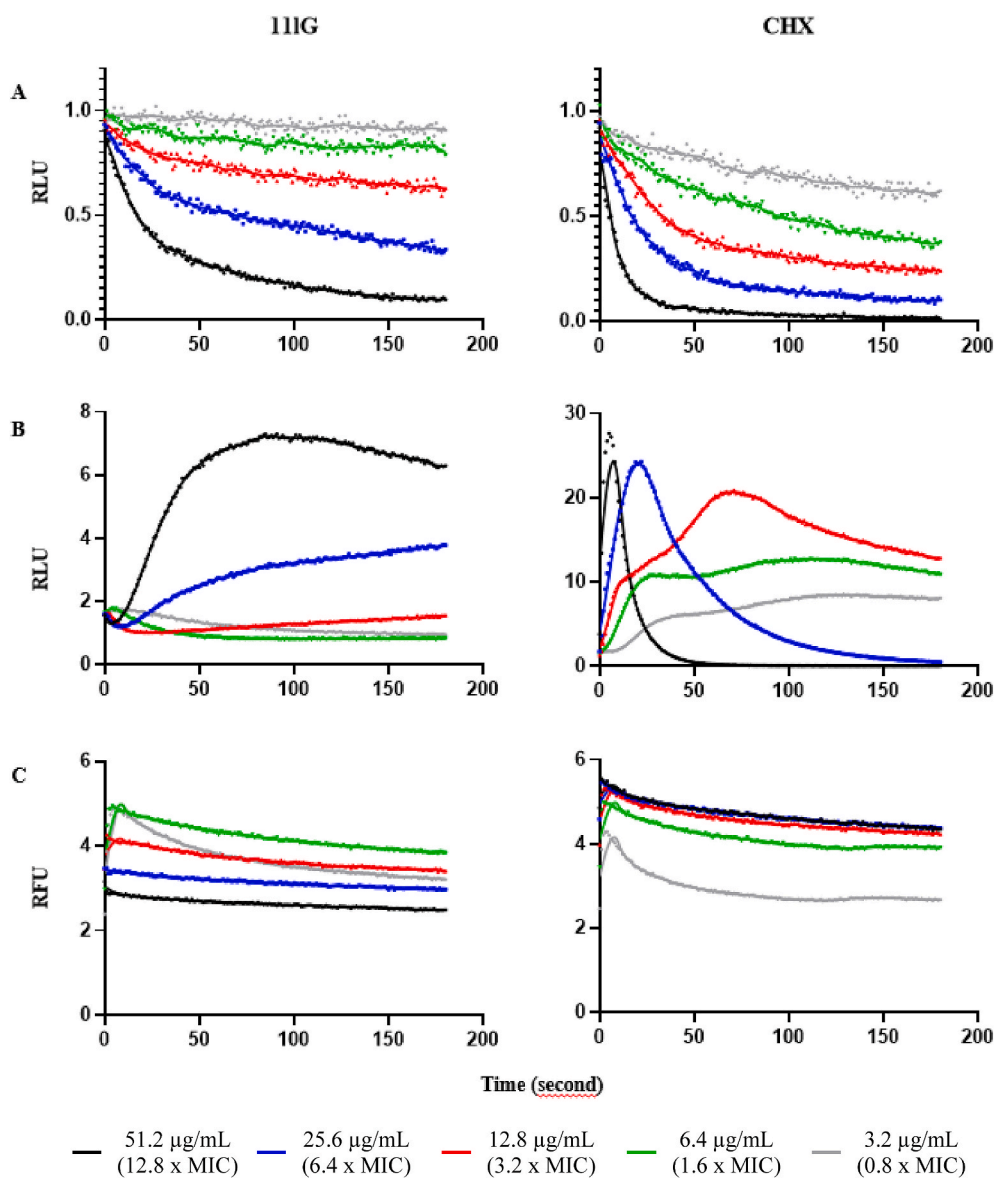


Fig. 5. The effects of **111G** (broad-spectrum) and a **CHX** (positive control) on the kinetics of (A) viability and (B) inner membrane integrity (C) outer membrane integrity in *E. coli* K12. Normalized light emission (normalized with a negative, untreated water control) is plotted as relative light units (RLU) over time (seconds) for A and B. For C, normalized fluorescence (normalized with a negative, untreated water control) is plotted as relative fluorescence units (RFU) over time (seconds). Light emission/fluorescence was measured each second for 180 s after adding the bacterial cell suspension (with 1 mM D-luciferin for the inner membrane integrity assay and 20 μ M 1-N-phenyl-naphthylamine for outer membrane integrity assay) to the analytes in separate wells. The multiples of the MIC values given in parentheses refers only to compound **111G**. The figure shows a representative data set from at least three independent experiments.

membrane disruptive effect was observed as only the two highest concentrations (6.4 – 12.8x MIC) gave a rise in light emission (and did not decline during the test period) (Fig. 5B, left). The delayed and reduced action of **111G** on the membrane integrity might be due to the outer membrane of *E. coli*, which probably acts as an additional barrier.

To confirm the assumption about the outer membrane barrier in *E. coli*, we used the 1-N-phenyl-naphthylamine (NPN) fluorescent probe to determine whether compound **111G** can affect the outer membrane to become more permeable. The small molecule NPN (219 Da) is weakly fluorescent in an aqueous solution, but when bound to phospholipids, it gives strong fluorescence [59]. The hydrophobic NPN cannot efficiently cross the outer membrane of intact *E. coli* cells, yielding low fluorescence, but if the outer membranes is compromised, NPN can reach the periplasmic space and bind phospholipids of the inner and outer membranes, thus producing increased fluorescence. In this assay, low concentrations (3.2 μ g/mL) of barbiturate **111G** led to higher fluorescence levels (Fig. 5C, left), but did not initially give any increase in luminescence in the inner membrane integrity assay (Fig. 5B, left). This phenomenon suggests that most of the cells are intact and viable without having significantly compromised integrity of the inner membrane but have increased permeability of the outer membrane. Upon increasing

the concentration of barbiturate **111G**, the fluorescence levels were lower (Fig. 5C, left) indicating either an intact outer membrane or rapid membrane disintegration before the start of the measurement. At the same time the viability of the bacterial cells was clearly reduced (Fig. 5A, left) and the inner membrane integrity was impaired (Fig. 5B, left).

When the 10 μ L sample of the NPN assay was spotted on an agar plate after the test period, the viability of the bacterial cells was clearly reduced for concentrations of 25.6–51.2 μ g/mL (6.4 – 12.8x MIC) (see Fig. S4), confirming the bactericidal effect of barbiturate **111G**. Those results strongly suggest that barbiturate **111G** disrupts both the outer and the inner membrane at the same rate when the concentration is high enough. However, it cannot be excluded that higher concentrations of **111G** induce a different mode of action, resulting in the compound crossing the outer membrane without disrupting it.

Our results indicate that the primary mode of action for most of the compounds, including the broad-spectrum barbiturate **111G**, against both the Gram-positive *B. subtilis* and the Gram-negative *E. coli*, is the disruption of the membrane integrity in a concentration-dependent manner. However, it is known that certain cationic AMPs exhibit a concentration-dependent dual mode of action [60]. For example, the

N-terminal 1–35 fragment of Bac7 (a proline-arginine-rich AMP) is known to affect the inner membrane at high concentrations and bind to and affect intracellular chaperone protein DnaK and 70S ribosomes at lower concentrations [61–63]. Therefore, there might also be other targets than the bacterial cytoplasmic membrane, and more work is required to conclude if there is any dual mode of action present or not.

3. Conclusion

In the present study, we have investigated the qualitative influence of the individual structural components of *N,N*-dialkylated-5,5-disubstituted amphipathic barbiturates on their bioactivity. We found that *n*-propyl linkers provide the best balance between antibacterial potency and haemolytic activity and *n*-butyl linkers provide the highest potency. Guanidyl head-groups led to the highest antimicrobial potency, whereas trimethylated amines proved to be attractive for narrow-spectrum application. By choosing the individual components carefully, we were able to prepare several compounds having SI values ≥ 20 and being active towards two (8a, 11kG, 13cG, 13hG), three (9a, 11IG, 13pG) or all four (13aG, 13iA, 13jA, 13jG) strains of our test panel. The best compounds (13aG, 13jG and 13jA) had an improved selectivity index compared to the initial starting point (1aG).

Studies on the integrity of the membranes and the viability of bacterial cells suggest that our compounds exert their bactericidal activity by disrupting the bacterial cell wall of Gram-positive *B. subtilis* in a concentration-dependent manner as exemplified by barbiturate 11IG. In Gram-negative *E. coli* both, the inner and outer membrane, were supposedly rapidly disrupted at higher compound concentration, but a second mechanism of action might be present in addition.

We believe that our detailed analysis can help to devise new amphipathic cationic mimics of antimicrobial peptides.

4. Experimental section

For a detailed description of all chemical and biological experimental procedures, chemical analysis, and supporting results, see the Supporting Information. Additional raw data is available through the DataverseNO repository, link: <https://doi.org/10.18710/GNTWOG>.

Author contributions

M.K.L., A.B. and M.B.S. designed the compound library; M.K.L and F. Z. performed the compound synthesis and analysis; A.R., H.D., H.-M.B., T.H. and K.S. determined the biological assays; A.R., H.D., T.A. performed the biological assays and M.K.L., A.R., H.D., H.-M.B., T.H., K.S., A.B. and M.B.S. analysed and interpreted the data. The manuscript was written through contributions of all authors. All authors have given approval to the final version of the manuscript.

Declaration of competing interest

The authors declare that they have no known competing financial interests or personal relationships that could have appeared to influence the work reported in this paper.

Data availability

Additional raw data is available through the DataverseNO repository, link: <https://doi.org/10.18710/GNTWOG>.

Acknowledgements

MKL, AR and HD thank for a PhD fellowship provided by UiT as part of the AntifoMar and LeadScAMR grants.

Appendix A. Supplementary data

Supplementary data to this article can be found online at <https://doi.org/10.1016/j.ejmech.2022.114632>.

References

- [1] M.I. Hutchings, A.W. Truman, B. Wilkinson, Antibiotics: past, present and future, *Curr. Opin. Microbiol.* 51 (2019) 72–80.
- [2] Global Action Plan on Antimicrobial Resistance, World Health Organization, Geneva, 2015.
- [3] P.D. Tamma, S.E. Cosgrove, L.L. Maragakis, Combination therapy for treatment of infections with gram-negative bacteria, *Clin. Microbiol. Rev.* 25 (2012) 450–470.
- [4] M. Laws, A. Shaaban, K.M. Rahman, Antibiotic resistance breakers: current approaches and future directions, *FEMS Microbiol. Rev.* 43 (2019) 490–516.
- [5] S.M. Mandal, A. Roy, A.K. Ghosh, T.K. Hazra, A. Basak, O.L. Franco, Challenges and future prospects of antibiotic therapy: from peptides to phages utilization, *Front. Pharmacol.* 5 (2014) 1–12.
- [6] M.R. Hamblin, T. Hasan, Photodynamic therapy: a new antimicrobial approach to infectious disease? *Photochem. Photobiol. Sci.* 3 (2004) 436–450.
- [7] A. DiGiandomenico, B.R. Sellman, Antibacterial monoclonal antibodies: the next generation? *Curr. Opin. Microbiol.* 27 (2015) 78–85.
- [8] N. Beyth, Y. Hourri-Haddad, A. Domb, W. Khan, R. Hazan, Alternative antimicrobial approach: nano-antimicrobial materials, *Evid. base Compl. Alternative Med.* 2015 (2015), 246012.
- [9] M.S. Mulani, E.E. Kamble, S.N. Kumkar, M.S. Tawre, K.R. Pardesi, Emerging strategies to combat ESKAPE pathogens in the era of antimicrobial resistance: a review, *Front. Microbiol.* 10 (2019) 1–24.
- [10] R.E. Hancock, A. Patrzykat, Clinical development of cationic antimicrobial peptides: from natural to novel antibiotics, *Curr. Drug Targets: Infect. Disord.* 2 (2002) 79–83.
- [11] M. Mahlapuu, J. Håkansson, L. Ringstad, C. Björn, Antimicrobial peptides: an emerging category of therapeutic agents, *Front. Cell. Infect. Microbiol.* 6 (2016) 1–12.
- [12] R.E.W. Hancock, H.-G. Sahl, Antimicrobial and host-defense peptides as new anti-infective therapeutic strategies, *Nat. Biotechnol.* 24 (2006) 1551–1557.
- [13] M. Pasupuleti, A. Schmidtchen, M. Malmsten, Antimicrobial peptides: key components of the innate immune system, *Crit. Rev. Biotechnol.* 32 (2012) 143–171.
- [14] M.R. Yeaman, N.Y. Yount, Mechanisms of antimicrobial peptide action and resistance, *Pharmacol. Rev.* 55 (2003) 27–55.
- [15] R.E.W. Hancock, Peptide antibiotics, *Lancet* 349 (1997) 418–422.
- [16] K.L. Brown, R.E.W. Hancock, Cationic host defense (antimicrobial) peptides, *Curr. Opin. Immunol.* 18 (2006) 24–30.
- [17] A. Ebbensgaard, H. Mordhorst, M.T. Overgaard, C.G. Nielsen, F.M. Aarestrup, E. B. Hansen, Comparative evaluation of the antimicrobial activity of different antimicrobial peptides against a range of pathogenic bacteria, *PLoS One* 10 (2015), e0144611.
- [18] K. Fosgerau, T. Hoffmann, Peptide therapeutics: current status and future directions, *Drug Discov. Today* 20 (2015) 122–128.
- [19] Y. Yang, Z. Cai, Z. Huang, X. Tang, X. Zhang, Antimicrobial cationic polymers: from structural design to functional control, *Polym. J.* 50 (2018) 33–44.
- [20] A. Strassburg, F. Kracke, J. Wenners, A. Jemeljanova, J. Kuepper, H. Petersen, J. C. Tiller, Nontoxic, hydrophilic cationic polymers—identified as class of antimicrobial polymers, *Macromol. Biosci.* 15 (2015) 1710–1723.
- [21] D. Liu, W.F. DeGrado, De novo design, synthesis, and characterization of antimicrobial β -peptides, *J. Am. Chem. Soc.* 123 (2001) 7553–7559.
- [22] P. Sang, Y. Shi, P. Teng, A. Cao, H. Xu, Q. Li, J. Cai, Antimicrobial A-peptides, *Curr. Top. Med. Chem.* 17 (2017) 1266–1279.
- [23] T. Hansen, T. Alst, M. Havelkova, M.B. Strøm, Antimicrobial activity of small β -peptidomimetics based on the pharmacophore model of short cationic antimicrobial peptides, *J. Med. Chem.* 53 (2010) 595–606.
- [24] P. Teng, A. Nimmagadda, M. Su, Y. Hong, N. Shen, C. Li, L.-Y. Tsai, J. Cao, Q. Li, J. Cai, Novel bis-cyclic guanidines as potent membrane-active antibacterial agents with therapeutic potential, *Chem. Commun.* 53 (2017) 11948–11951.
- [25] M.H. Paulsen, E.A. Karlens, D. Ausbacher, T. Anderssen, A. Bayer, P. Ochtrup, C. Hedberg, T. Haug, J.U. Ericson Sollid, M.B. Strøm, An amphipathic cyclic tetrapeptide scaffold containing halogenated $\beta^{2,2}$ -amino acids with activity against multidrug-resistant bacteria, *J. Pept. Sci.* 24 (2018) e3117.
- [26] M.H. Paulsen, D. Ausbacher, A. Bayer, M. Engqvist, T. Hansen, T. Haug, T. Anderssen, J.H. Andersen, J.U.E. Sollid, M.B. Strøm, Antimicrobial activity of amphipathic α,α -disubstituted β -amino amide derivatives against ESBL – CARBA producing multi-resistant bacteria; effect of halogenation, lipophilicity and cationic character, *Eur. J. Med. Chem.* 183 (2019), 111671.
- [27] M. Wang, X. Feng, R. Gao, P. Sang, X. Pan, L. Wei, C. Lu, C. Wu, J. Cai, Modular design of membrane-active antibiotics: from macromolecular antimicrobials to small scorpionlike peptidomimetics, *J. Med. Chem.* 64 (2021) 9894–9905.
- [28] M.H. Paulsen, M. Engqvist, D. Ausbacher, T. Anderssen, M.K. Langer, T. Haug, G. R. Morello, L.E. Liikanen, H.-M. Blencke, J. Isaksson, E. Juskevicius, A. Bayer, M. B. Strøm, Amphipathic barbiturates as mimics of antimicrobial peptides and the marine natural products eusynstyelamides with activity against multi-resistant clinical isolates, *J. Med. Chem.* 64 (2021) 11395–11417.
- [29] D.M. Tapiolas, B.F. Bowden, E. Abou-Mansour, R.H. Willis, J.R. Doyle, A. N. Muirhead, C. Liprot, L.E. Llewellyn, C.W. Wolff, A.D. Wright, C.A. Motti,

- B. Eusynstyelamides A, C. nNOS inhibitors, From the ascidian Eusynstyela latericius, *J. Nat. Prod.* 72 (2009) 1115–1120.
- [30] M. Tadesse, J.N. Tabudravu, M. Jaspars, M.B. Strom, E. Hansen, J.H. Andersen, P. E. Kristiansen, T. Haug, The antibacterial ent-eusynstyelamide B and eusynstyelamides D, E, and F from the Arctic bryozoan *Tegella cf. spitzbergensis*, *J. Nat. Prod.* 74 (2011) 837–841.
- [31] M.F. Richter, B.S. Drown, A.P. Riley, A. Garcia, T. Shirai, R.L. Svec, P. J. Hergenrother, Predictive compound accumulation rules yield a broad-spectrum antibiotic, *Nature* 545 (2017) 299–304.
- [32] S.J. Perlmutter, E.J. Geddes, B.S. Drown, S.E. Motika, M.R. Lee, P.J. Hergenrother, Compound uptake into *E. coli* can be facilitated by N-alkyl guanidiniums and pyridiniums, *ACS Infect. Dis.* 7 (2021) 162–173.
- [33] S. Zhang, Z. Shi, W. Cao, T. Gao, H. Deng, Synthesis of a series of perfluoroalkyl containing spiro cyclic barbituric acid derivatives, *J. Chem. Res.* 2009 (2009) 381–383.
- [34] S. Kotha, A.C. Deb, R.V. Kumar, Spiro-annulation of barbituric acid derivatives and its analogs by ring-closing metathesis reaction, *Bioorg. Med. Chem. Lett.* 15 (2005) 1039–1043.
- [35] K.T. Mahmudov, M.N. Kopylovich, A.M. Maharramov, M.M. Kurbanova, A. V. Gurbanov, A.J.L. Pombeiro, Barbituric acids as a useful tool for the construction of coordination and supramolecular compounds, *Coord. Chem. Rev.* 265 (2014) 1–37.
- [36] J.T. Bojarski, J.L. Mokrosz, H.J. Bartoń, M.H. Paluchowska, Recent progress in barbituric acid chemistry, in: A.R. Katritzky (Ed.), *Adv. Heterocycl. Chem.*, Academic Press, 1985, pp. 229–297.
- [37] J.V. Tate, W.N. Tinnerman II, V. Jurevics, H. Jeskey, E.R. Biehl, Preparation of 5-substituted benzylbarbituric acids and investigation of the effect of the benzyl and substituted benzyl groups on the acidity of barbituric acid, *J. Heterocycl. Chem.* 23 (1986) 9–11.
- [38] D.B. Ramachary, M. Kishor, Y.V. Reddy, Development of pharmaceutical drugs, drug intermediates and ingredients by using direct organo-click reactions, *Eur. J. Org. Chem.* 2008 (2008) 975–993.
- [39] S.J. Kalita, D.C. Deka, 2-Phenyl-2,3-dihydrobenzo[d]thiazole: a mild, efficient, and highly active in situ generated chemoselective reducing agent for the one-pot synthesis of 5-monoalkylbarbiturates in water, *Synlett* 29 (2018) 477–482.
- [40] J.D. Figueroa-Villar, E.R. Cruz, N. Lucia dos Santos, Synthesis of oxadiazaflavines from barbituric acid and aromatic aldehydes, *Synth. Commun.* 22 (1992) 1159–1164.
- [41] A.A. Vieira, B.G. Marinho, L.G. de Souza, P.D. Fernandes, J.D. Figueroa-Villar, Design, synthesis and in vivo evaluation of sodium 2-benzyl-chloromalonates as new central nervous system depressants, *MedChemComm* 6 (2015) 1427–1437.
- [42] S. Fletcher, The Mitsunobu reaction in the 21st century, *Org. Chem. Front.* 2 (2015) 739–752.
- [43] A.R. Katritzky, B.V. Rogovoy, Recent developments in guanylating agents, *Archive for Organic Chem.* 2005 (2005) 49–87.
- [44] T. Gers, D. Kunce, P. Markowski, J. Izdebski, Reagents for efficient conversion of amines to protected guanidines, *Synthesis* 2004 (2004) 37–42.
- [45] K. Midura-Nowaczek, A. Markowska, Antimicrobial peptides and their analogs: searching for new potential therapeutics, *Perspect. Med. Chem.* 6 (2014) 73–80.
- [46] J.S. Dickson, M. Koohmarai, Cell surface charge characteristics and their relationship to bacterial attachment to meat surfaces, *Appl. Environ. Microbiol.* 55 (1989) 832–836.
- [47] G.M. Bruinsma, M. Rustema-Abbing, H.C. van der Mei, C. Lakkis, H.J. Busscher, Resistance to a polyquaternium-1 lens care solution and isoelectric points of *Pseudomonas aeruginosa* strains, *J. Antimicrob. Chemother.* 57 (2006) 764–766.
- [48] A. Skrzypczak, B. Brycki, I. Mirska, J. Pernak, Synthesis and antimicrobial activities of new quats, *Eur. J. Med. Chem.* 32 (1997) 661–668.
- [49] F. Devínský, I. Lacko, F. Bittererová, D. Mlynářčík, Quaternary ammonium-salts. 18. Preparation and relationship between structure, IR spectral characteristics, and antimicrobial activity of some new bis-quaternary isomers of 1,5-pentanediammonium dibromides, *Chem. Pap.* 6 (1987) 803–814.
- [50] P. Gilbert, L.E. Moore, Cationic antiseptics: diversity of action under a common epithet, *J. Appl. Microbiol.* 99 (2005) 703–715.
- [51] T. Hansen, M.K. Moe, T. Anderssen, M.B. Strøm, Metabolism of small antimicrobial β 2,2-amino acid derivatives by murine liver microsomes, *Eur. J. Drug Metab. Pharmacokinet.* 37 (2012) 191–201.
- [52] E.P. Gillis, K.J. Eastman, M.D. Hill, D.J. Donnelly, N.A. Meanwell, Applications of fluorine in medicinal chemistry, *J. Med. Chem.* 58 (2015) 8315–8359.
- [53] D.H. McDaniel, H.C. Brown, An extended table of hammett substituents constants based on the ionization of substituted benzoic acids, *J. Org. Chem.* 23 (1958) 420–427.
- [54] D. Gupta, D. Bhatia, V. Dave, V. Sutariya, S. Varghese Gupta, Salts of therapeutic agents: chemical, physicochemical, and biological considerations, *Molecules* 23 (2018) 1719.
- [55] A.T.M. Serajuddin, Salt formation to improve drug solubility, *Adv. Drug Deliv. Rev.* 59 (2007) 603–616.
- [56] P.L. Gould, Salt selection for basic drugs, *Int. J. Pharm.* 33 (1986) 201–217.
- [57] M. Virta, K.E.O. Åkerman, P. Saviranta, C. Oker-Blom, M.T. Karp, Real-time measurement of cell permeabilization with low-molecular-weight membranolytic agents, *J. Antimicrob. Chemother.* 36 (1995) 303–315.
- [58] T. Kuyyakanond, L.B. Quesnel, The mechanism of action of chlorhexidine, *FEMS Microbiol. Lett.* 100 (1992) 211–215.
- [59] B. Loh, C. Grant, R.E. Hancock, Use of the fluorescent probe 1-N-phenyl-naphthylamine to study the interactions of aminoglycoside antibiotics with the outer membrane of *Pseudomonas aeruginosa*, *Antimicrob. Agents Chemother.* 26 (1984) 546–551.
- [60] M. Graf, M. Mardrossian, F. Nguyen, A.C. Seefeldt, G. Guichard, M. Scocchi, C. A. Innis, D.N. Wilson, Proline-rich antimicrobial peptides targeting protein synthesis, *Nat. Prod. Rep.* 34 (2017) 702–711.
- [61] E. Podda, M. Benincasa, S. Pacor, F. Micali, M. Mattiuzzo, R. Gennaro, M. Scocchi, Dual mode of action of Bac7, a proline-rich antibacterial peptide, *Biochim. Biophys. Acta* 1760 (2006) 1732–1740.
- [62] M.L. Scocchi, P. Decarli, G. Mignogna, P. Christen, R. Gennaro, The proline-rich antibacterial peptide Bac7 binds to and inhibits in vitro the molecular chaperone DnaK, *Int. J. Pept. Res. Therapeut.* 15 (2009) 147–155.
- [63] M. Mardrossian, R. Grzela, C. Giglione, T. Meinel, R. Gennaro, P. Mergaert, M. Scocchi, The host antimicrobial peptide Bac71-35 binds to bacterial ribosomal proteins and inhibits protein synthesis, *Chem. Biol.* 21 (2014) 1639–1647.